Eur. Phys. J. D **8**, 85–91 (2000)

THE EUROPEAN PHYSICAL JOURNAL D
EDP Sciences

Doublet and quartet states of Li_2^-

H. Hogreve[a]

Centre de Physique Théorique, CNRS, Luminy Case 907, 13288 Marseille Cedex 9, France

Received 23 March 1999

Abstract. Electronic states of the molecular lithium anion are investigated by configuration-interaction calculations. Comparison with the analogously computed potential energy curves for the lowest singlet and triplet states of the neutral Li_2 shows that in addition to the well-known stable ground state $X^2\Sigma_u^+$ there also exist metastable excited states of Li_2^-. Within the quartet sector, two candidates for such long-lived states are identified and their spectroscopic properties studied.

PACS. 31.15.Ar Ab initio calculations – 33.15.Fm Bond strengths, dissociation energies – 33.15.Dj Interatomic distances and angles

1 Introduction

Not all of the elements lead to stable atomic anions, and even fewer homonuclear diatomic molecules are capable of forming stable negative molecular ions. Since neither H_2^- nor He_2^- has a bound ground state, Li_2^- is the smallest homonuclear anion that exhibits stability. Theoretically, the stability of the ground state $X^2\Sigma_u^+$ of Li_2^- was already predicted in 1972 [1]; its experimental detection, however, was not reported until two decades later [2]. The original results [1] have been refined by a series of subsequent calculations [3–11], so that currently for the ground state $X^2\Sigma_u^+$ there is a satisfactory agreement between the published theoretical and published experimental data.

Less information, both quantitatively and qualitatively, is available for excited states of Li_2^-. Usually, atomic anions have no or only a very few bound excited states below their electron detachment thresholds. In particular, there are no excited bound states for Li^-, and, if considering a general nuclear charge parameter Z, all bound states of the four-electron atomic system will be absorbed into the continuous spectrum if $Z < 2.85e_0$ [12]. On the other hand, the system that would arise in the united-atom limit (UAL) of Li_2^-, namely the carbon anion C^-, enjoys two bound states: in addition to its ground state $^4S^o$, the excited state $^2D^o$ is weakly bound by ≈ 0.036 eV [13]. These facts already indicate that isolated (*i.e.* lying below the continuum) excited bound states should be rather scarce for Li_2^-. Actually, previous studies [7–9] only predict the lowest excited state $1^2\Sigma_g^+$ to be bound for large internuclear separations R, *viz.* $R > 6.5a_0$. Experimentally, the resulting spectral properties render this state $1^2\Sigma_g^+$ an attractive candidate for dissociative electron attachment measurements [14].

Although in principle quartet or higher spin states of Li_2^- could acquire a rather long lifetime, they have not yet been discussed in the literature. A sufficiently small spin-orbit coupling is one of the prerequisites for the metastability of such states. Another stability condition for a spin S state of Li_2^- is that its energy (or, more precisely, a minimum of its associated Born-Oppenheimer potential energy curve (PEC)) lies below the bottom of the corresponding spin $(S-1)$ spectrum of Li_2. If Hund's case b coupling scheme and thus the rule $\Delta S = \pm 1$ for single-electron detachment were strictly valid, that energy requirement would entail not only metastability, but genuine stability. In reality, however, states stabilized in this way eventually decay, with their lifetime being determined by the strength of the interaction terms neglected. The state $1^4\Pi_u$ of N_2^- discussed recently in reference [15] provides an example for a quartet state that is energetically above but much ($> 10^7$ times) longer lived than the lower doublet states of N_2^-.

Here, our main goal is to study the low-lying quartet spectrum of Li_2^- and to identify candidates for metastable states. This also includes a reinvestigation of the relevant ionic doublet and neutral threshold states.

2 Computational details

Due to the extra electron in Li_2^- the anionic states can be expected to be represented by spatially rather extended and diffuse wave functions. This motivates the addition of appropriate polarization functions for building an adequate Li_2^- basis from a given basis set for Li_2. The main impact of these polarization functions will be an improved description of the loosely bound electron

---

[a] *Permanent address*: IFISR, Freiheit 13, 31174 Schellerten, Germany. e-mail: `hogreve@rz.uni-hildesheim.de` or e-mail: `hogreve@cpt.univ-mrs.fr`

of the anionic wave function; therefore, application of a basis set constructed in such a way to both the ion Li_2^- and the neutral Li_2 systems should allow a fairly consistent determination of the stability properties of Li_2^-.

Guided by these considerations and having experimented with various basis sets, most of our calculations were performed using a Gaussian basis with sets $(14s7p5d2f)$ attached to each nucleus and amended by a set $(3s1p)$ at the bond centre. Since, to achieve maximal flexibility, all functions were kept uncontracted, this yields a total number of 176 basis functions and thus a basis of much larger size than in previous investigations on these systems [1,3–11,16–25]. The employed set of s-orbitals is derived from Table 3.14.1 in reference [26]; apart from additional p- and d-functions with exponents $\zeta_p = 45.0$ and $\zeta_d = 0.038$, respectively, the p-, d-, and f-sets are identical to the corresponding ones of the Li-basis in reference [27].

Our CI calculations adhere to the standard MRDCI scheme [28]. Depending on the state and the actual geometry, usually between 30 and 60 reference configurations were specified and produced a set of several million symmetry adapted functions. Selection thresholds between 0.1 and 0.4 μhartree led to dimensions of the Hamilton matrix ranging from 12 to 55 thousand. After computation of its lowest eigenvalues and construction of the corresponding natural orbitals, the CI procedure was repeated iteratively, usually with distinctly smaller selection thresholds. In this way, the contributions $\sum_n c_n^2$ of the reference configurations to the final CI wave function were enhanced by $\approx 1-2\%$, reaching 98.8–99.4% for the CINO wave functions of Li_2^- or 99.2–99.6% for Li_2. Here, and in the sequel, the notation CINO refers to results from MRDCI computations with natural orbitals, and CINOQ will indicate that in addition the generalized Davidson correction [29] was employed. Besides computations in which all electrons are correlated, also calculations with frozen-core $1\sigma_g^2 1\sigma_u^2$ have been carried out. For both the neutral and ionic system, on the average, the resulting total energies were ≈ 88 mHartree above the respective values from the all-electron computations. As expected, freezing orbitals increases the contribution $\sum_n c_n^2$ of the reference sets to $\approx 99.9\%$ for Li_2 or 99.1–99.9% in the case of Li_2^-.

3 Potential energy curves for Li_2

In the context of studying Li_2^-, a (re-)computation of PECs for its neutral parent Li_2 is desirable for two principal reasons. First, the energies of certain Li_2 states determine the respective thresholds for electron detachment from Li_2^-; hence, even though some relevant data are already available in the literature, calculations employing the same basis and CI method for both the neutral and the ionic molecule should provide more consistent and thus more accurate stability information on Li_2^-. Secondly, comparison of our computed Li_2 data with other precise results allows some calibration and more reliable accuracy estimates for our computed Li_2^- quantities also.

Among the previous theoretical studies that cover the required states, we should mention in particular the investigations by Kaldor [24] and by Schmidt-Mink *et al.* [23]. Kaldor's results are purely *ab initio*, whereas for the data in reference [23] a semiempirical effective potential is used to include core polarization effects. Theoretical and experimental results are collected and compared with values from our computations in Table 1 for the three states of Li_2 that mark the considered Li_2^- thresholds. For the ground state $\mathrm{X}^1\Sigma_g^+$ the experimental spectroscopic constants ω_e and D_e are most closely reproduced by the recent calculations of Evangelisti *et al.* [25]. The theoretical R_e values from reference [6] or from reference [23] are $0.004a_0$ below or above, respectively, of the experimental equilibrium bond length R_e; our CINO PEC yields an equilibrium separation that is $0.006a_0$ larger than the one from experiments. The CCPCI [23] and our CINO computations produce an identical result for the dissociation energy D_e, the predicted value being about 1% smaller than the experimental D_e. With the exception of the anharmonicity parameter $\omega_\mathrm{e}x_\mathrm{e}$ for which the CINOQ-PEC gives $\omega_\mathrm{e}x_\mathrm{e} = 2.80\ \mathrm{cm}^{-1}$, our Davidson-corrected CINOQ results deviate less than 0.3% from the uncorrected CINO-values; however, they are less consistent with the experiment. In their CI calculations, Partridge *et al.* [6] observed that freezing the orbitals $1\sigma_g^2 1\sigma_u^2$ leads to an equilibrium separation R_e elongated by $\approx 0.04a_0$ with respect to the all-electron treatment; the same phenomenon occurs in our computations. For other quantities, we found that freezing the $1\sigma_g^2 1\sigma_u^2$ core results in smaller values, *i.e.*, 0.7% for D_e and 1.7% for ω_e.

Since their associated PECs cross around $R_x = 4.82a_0$, we have to consider two states, *viz.* $1^3\Sigma_u^+$ and $1^3\Pi_u$, to obtain the lowest triplet energies for Li_2. These states converge to different separated atoms limits (SALs); the state $1^3\Sigma_u^+$ dissociates into $\mathrm{Li}(2s\,^2\mathrm{S}) + \mathrm{Li}(2s\,^2\mathrm{S})$ and its PEC is the lower one for $R > R_x$, whereas $1^3\Pi_u$ produces $\mathrm{Li}(2s\,^2\mathrm{S}) + \mathrm{Li}(2p\,^2\mathrm{P})$ as $R \to \infty$. Experimental data are available for the state $1^3\Pi_u$, but not for $1^3\Sigma_u^+$. As Table 1 shows, for $1^3\Pi_u$ most of the theoretical results agree rather well with the experimental ones. The minimum of the $1^3\Pi_u$ PEC arises at a separation R_e that is larger than the crossing R_x. Hence, in the present context, only the repulsive part $R \leq R_x < R_\mathrm{e}$ of the $1^3\Pi_u$ PEC will be of interest.

Probably due to its shallow well and small D_e, the state $1^3\Sigma_u^+$ has not yet been observed in experiments. Those weak binding properties are certainly also the reason for a less consistent theoretical description of the $1^3\Sigma_u^+$ PEC. The deviations are most striking for the equilibrium separation R_e, with CI results scattered between 7.55 and $7.90a_0$. Minor discrepancies exist for T_e, but for D_e our CINO value is about 20% smaller than the average of the other CI values in Table 1.

4 Doublet states of Li_2^-

In the separated atoms limit (SAL), the channel with lowest energy is characterized by the dissociation products $\mathrm{Li}^-(^1\mathrm{S}_g) + \mathrm{Li}(^2\mathrm{S}_g)$. Only the two molecular states $\mathrm{X}^2\Sigma_u^+$

Table 1. Spectroscopic constants for those states of Li_2 that are of relevance for the stability of the molecular anion Li_2^-. In addition to the standard abbreviations, the employed methods are indicated by: EXP: experiment; CINO: MRDCI with natural orbitals; CCSD: coupled clusters with single and double excitations; CPP CI: effective core polarization potential and full valence CI; BPP CI: Bardley's pseudo-potential and valence CI.

state	method	reference	R_e/a_0	T_e/cm^{-1}	$\omega_e/\mathrm{cm}^{-1}$	$\omega_e x_e/\mathrm{cm}^{-1}$	D_e/eV
$X^1\Sigma_g^+$	EXP	[30,31]	5.051	0	351.39	2.578	1.0559
	CINO	(a)	5.057	0	351.2	2.40	1.045
	CAS CI	[25]	5.042	0	351.96	-	1.0561
	CCSD	[24]	5.05	0	351	-	1.061
	CPP CI	[23]	5.055	0	351.01	2.586	1.045
	MCSCF CI	[6]	5.047	0	350.5	2.58	1.034
	BPP CI	[22]	5.002	0	356.9	3.66	1.078
$1^3\Sigma_u^+$	CINO	(a)	7.55	8191	69.8	4.8	0.0329
	CCSD	[24]	7.65	8251	75	-	0.0380
	CPP CI	[23]	7.903	8144	63.73	3.202	0.0399
	BPP CI	[22]	7.687	-	66.4	3.11	0.0439
	MCSCF	[17]	8.001	-	61	3.2	0.0362
$1^3\Pi_u$	EXP	[32]	4.894	-	345.6	1.890	1.5058
	EXP	[33]	4.896	11240	345.7	-	1.510
	CINO	(a)	4.893	11345	348.3	1.92	1.510
	CCSD	[24]	4.88	11090	349	-	1.533
	CPP CI	[23]	4.904	11257	345.88	1.980	1.5061
	BPP CI	[22]	4.828	-	354.1	2.52	1.5427
	MCSCF	[18]	4.974	-	339	2.5	1.4237
(a) this work							

Table 2. Spectroscopic constants for stable or metastable states of Li_2^-.

state $X^2\Sigma_u^+$	dominant configuration $1\sigma_g^2 1\sigma_u^2 2\sigma_g^2 2\sigma_u$					
method	reference	R_e/a_0	$\omega_e/\mathrm{cm}^{-1}$	$\omega_e x_e/\mathrm{cm}^{-1}$	D_e/eV	D_0/eV
EXP	[2]	5.847	232	-	-	0.865
CINO	(a)	5.819	232.2	2.30	0.844	0.830
CINOQ	(a)	5.787	236.8	2.42	0.857	0.842
CAS CI	[10]	5.85	230	-	-	0.75 (0.83)(b)
CI	[9]	5.813	231.3	2.36	0.7084	0.818
MP CI	[7]	5.644	233.1	1.92	0.880	-
SDTCI	[8]	5.840	230.4	2.15	0.794	-
MCSCF CI	[6]	5.779	231.2	2.31	0.907 (0.836)(b)	-
state $1^4\Sigma_u^+$	dominant configuration $1\sigma_g^2 1\sigma_u^2 2\sigma_g 2\sigma_u 3\sigma_g$					
method	R_e/a_0	T_e/cm^{-1}	T_v/cm^{-1}	$\omega_e/\mathrm{cm}^{-1}$	$\omega_e x_e/\mathrm{cm}^{-1}$	$\mathrm{EA_a}/\mathrm{eV}$
CINO	6.570	9335	9709	157.2	1.53	0.246
CINOQ	6.577	9309	9731	166.1	2.01	0.257
state $1^4\Pi_g$	dominant configuration $1\sigma_g^2 1\sigma_u^2 2\sigma_g 2\sigma_u 3\sigma_g$					
method	R_e/a_0	T_e/cm^{-1}	T_v/cm^{-1}	$\omega_e/\mathrm{cm}^{-1}$	$\omega_e x_e/\mathrm{cm}^{-1}$	$\mathrm{EA_a}/\mathrm{eV}$
CINO	5.901	10071	10074	191.9	2.01	0.156
CINOQ	5.899	10043	10047	198.7	2.48	0.163
(a) this work						
(b) Davidson corrected value						

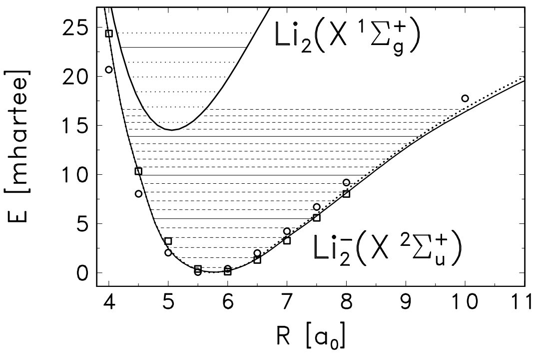

Fig. 1. PECs from CINO results (solid lines) for the ground state $X^2\Sigma_u^+$ of Li_2^- and ground state $X^1\Sigma_g^+$ of Li_2. Inside of the PECs the lowest twenty (for $^7Li_2^-$) or seven (for $^7Li_2$) vibrational levels are indicated. For Li_2^-, the CINO PEC is also compared with the CINOQ results (dotted curve) or with (relative) energies from other calculations (circles: Ref. [7]; squares: Ref. [9]). All PECs are drawn relative to their respective minimum.

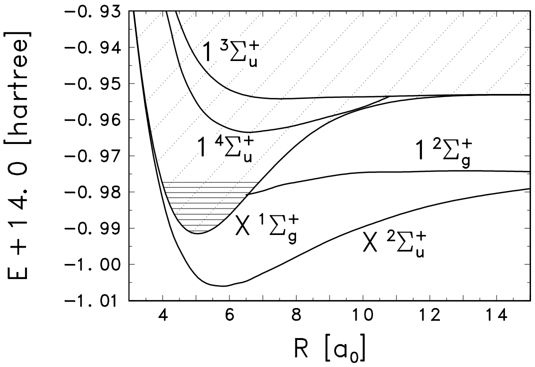

Fig. 2. Nondetaching doublet states and lowest quartet state of Li_2^- together with relevant threshold states of Li_2. The doublet continuum is indicated by shadowing, and inside the $X^1\Sigma_g^+$ PEC the lowest ten vibrational levels for $^7Li_2$ are displayed.

and $1^2\Sigma_g^+$ converging to that limit remain electronically stable for large internuclear separations, because the first excited SAL channel corresponds to $Li^-(^3P_u)$ + $Li(^2S_g)$ and $Li^-(^3P_u(1s^22s2p))$ is not bound. In the UAL, the two bound states $^4S^o$ and $^2D^o$ correlate with the molecular states $1^4\Sigma_g^-$ and $1^2\Pi_u$, respectively. This implies that in Li_2^- the state $X^2\Sigma_u^+$ must lose its ground state privilege due to a crossing with $1^4\Sigma_g^-$ for small R. Our calculations, however, reveal that for internuclear separations larger than $\approx 3a_0$ – and thus for the domain of primary interest – the $X^2\Sigma_u^+$ PEC is the lowest one. This PEC together with the ground state $X^1\Sigma_g^+$ PEC of Li_2 is plotted in Figure 1. Spectroscopic constants for $X^2\Sigma_u^+$ from our and other calculations are collected in Table 2. Compared with the ground state PEC of Li_2, the $X^2\Sigma_u^+$ well is rather shallow around its minimum. This explains the less coherent CI results for R_e between 5.65 and $5.85a_0$ in the case of Li_2^-; also the CINO and CINOQ values for R_e differ by $\approx 0.03a_0$. Nevertheless, the theoretical results from references [8,10] and our CINO value fall within the experimental error bars $R_e = 5.847 \pm 0.028a_0$ [2].

The dominant configuration for $X^2\Sigma_u^+$ is obtained by adding an $2\sigma_u$ orbital to the ground state configurations of neutral Li_2. The fact that the extra electron occupies an antibonding orbital is the reason for many of the differences between the ground state PECs of Li_2^- and Li_2, in particular the wider well for $X^2\Sigma_u^+$, the ≈ 20% smaller well depth and the $\approx 0.8a_0$ larger bond length of Li_2^-. The theoretical values for the well depth, *i.e.*, the dissociation energy D_e, range from 0.71 to 0.91 eV. Sarkas *et al.* [2] derived from their measured electron affinity for Li_2 the dissociation energy (including zero-point correction) $D_0 = 0.865 \pm 0.022$ eV for Li_2^-. The computed D_0 in Table 2 are smaller; only the CINOQ result hits the lower boundary of the experimental error interval.

The vibrational levels indicated in Figure 1 show that the $v = 17$ level of Li_2^- closely approximates the $v = 0$ level of Li_2. Hence, in addition to vibrational de-excitation, levels of the anion with $v \geq 17$ can also decay *via* electron detachment into $Li_2(X^1\Sigma_g^+)+e^-$. The quantities of importance for electron capture of Li_2 or electron detachment of Li_2^- are collected in Table 3.

Next, examining excited doublet states, the stability of the state $1^2\Sigma_g^+$ is lost for shorter internuclear separations before an equilibrium geometry is achieved due to the crossing of the $1^2\Sigma_g^+$ PEC with the continuum threshold curve $X^1\Sigma_g^+$ of Li_2 at $R_x \approx 6.5a_0$ (see Tab. 4 and Fig. 2). In terms of vibrational levels, the crossing energy corresponds to $v = 6$–7 of $^7Li_2$. For Be_2^+, a local maximum of the $1^2\Sigma_g^+$ PEC was observed around $R_b \approx 6.2a_0$ [27,34,35]; for Li_2^-, the maximum is shifted to much larger internuclear separations. The $1^2\Sigma_g^+$ PECs from our computations show a tiny hump around $R_b = 13a_0$; whereas existence of such a hump is independent of the employed computational method, its precise location and size are rather sensitive to details of the PEC.

Since the dipole transition probability $X^2\Sigma_u^+ \longleftarrow 1^2\Sigma_g^+$ is nonvanishing, the state $1^2\Sigma_g^+$ can decay by radiative processes; for $R_x < R < R_b$, our computations yield corresponding lifetimes between 0.5 and 3 microseconds. For $R < R_x$, the state $1^2\Sigma_g^+$ turns into a resonance. Some of its properties were investigated by Michels *et al.* [9]. In particular, the lifetime of this resonance is estimated to be long enough to admit dissociative attachment processes $Li_2(X^1\Sigma_g^+) + e^- \longrightarrow Li_2^-(1^2\Sigma_g^+) \longrightarrow Li(^2S) + Li^-(^1S)$ provided the initial electronic ground state of Li_2 is populated by sufficiently excited vibronic levels. Our computations predict thresholds for the dissociative attachment (relative to the $X^1\Sigma_g^+$ minimum) of 3619 cm^{-1} (CINO), or 3645 cm^{-1} (CINOQ), or the smaller frozen-core result 3457 cm^{-1}. In all cases, these values fall between the vibrational levels $v = 10$ and $v = 11$ for $^7Li_2$, consistent with the experimental findings [14].

Table 3. Adiabatic electron affinity EA_a, vertical electron affinity EA_v, and vertical detachment energy DE_v for the ground state of Li_2^-.

method	reference	EA_a / eV	EA_v / eV	DE_v / eV
EXP	[2]	0.437 ±0.009	-	0.52
CINO	(a)	0.402 (0.395)$^{(b)}$	0.328	0.492
CINOQ	(a)	0.416 (0.409)$^{(b)}$	0.341	0.502
VCINO	(a)	0.430 (0.423)$^{(b)}$	0.341	0.500
CAS CI	[25]	0.414	-	0.515
CI	[9]	0.42	-	-
BPP CI	[22]	0.429	-	-
SDTCI	[8]	0.44	0.37	0.50
MCSCF CI	[6]	0.43 ±0.02	-	-

no entry means: value not reported

(a) this work

(b) values in brackets: without zero-point motion

Table 4. Crossing point R_x with $\mathrm{X}^1\Sigma_g^+$ PEC of Li_2, energy $T_x = E(R_x) - E(R_\mathrm{e})$ at crossing relative to the minimum of the $\mathrm{X}^1\Sigma_g^+$ PEC, position R_b of barrier and barrier height E_b for the state $1^2\Sigma_g^+$ of Li_2^-.

method	reference	R_x/a_0	T_x/eV	R_b/a_0	$E_\mathrm{b}/\mathrm{cm}^{-1}$
CINO	(a)	6.56	0.2966	13.02	199
CINOQ	(a)	6.51	0.2726	13.18	208
VCINO	(a)	6.49	0.2551	13.20	126
VCINOQ	(a)	6.48	0.2520	13.20	128
CI	[9]	6.52	0.2730	12.21	201
BPP CI	[22]	6.21	0.2186	13.14	93
SDTCI	[8]	6.50	0.238	11.0	242

(a) this work

5 Quartet states of Li_2^-

The considerations of the preceding sections suggest that on the R-interval decisive for molecular stability the quartet states of Li_2^- are within the electronic continuum above the $\mathrm{X}^1\Sigma_g^+$ threshold. Assuming strict validity of the Hund's case b coupling scheme, the threshold for electron detachment of quartet states, however, is determined by the bottom of the triplet spectrum of Li_2. On the other hand, since the $1^3\Sigma_u^+$ energies of Li_2 converge to the same SAL as its $\mathrm{X}^1\Sigma_g^+$ PEC, from the beginning it is clear that for sufficiently large internuclear separations R all quartet states must become electronically unstable even under the strict spin-coupling assumption. Therefore, (meta)stable quartet states of Li_2^- can only be possible for small or moderate bond lengths. The actual behaviour of the PECs as predicted by our computations is displayed in Figure 3.

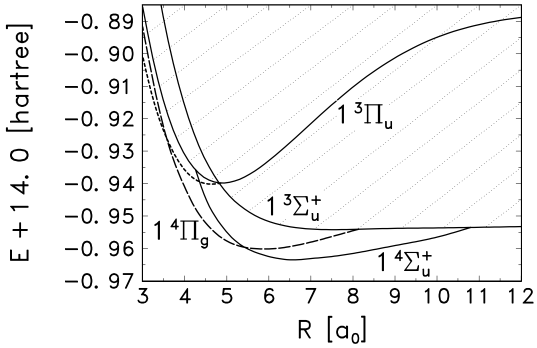

Fig. 3. Quartet states of Li_2^- and threshold states of Li_2 with the quartet continuum indicated by shadowing. The short-dashed curve represents the part of the $1^4\Sigma_g^-$ PEC below the continuum.

If ordered according to increasing energy, for the low-lying quartet states of Be_2^+ the sequence $1^4\Sigma_u^+$, $1^4\Pi_g$, $1^4\Pi_u$, $1^4\Sigma_g^+$ was found [27,35]. Our results yield the same energetic ordering also for the quartet states of Li_2^-. The global minimum of the discrete quartet spectrum of Li_2^- occurs for the state $1^4\Sigma_u^+$ at $R_\mathrm{e} = 6.57a_0$. The domain of (meta)stability for this state, *i.e.* the R-interval on which the $1^4\Sigma_u^+$ PEC stays below the electronic quartet continuum, ranges from $R_x(1^4\Sigma_u^+, 1^3\Pi_u) = 4.25a_0$ to $R_x(1^4\Sigma_u^+, 1^3\Sigma_u^+) = 10.94a_0$. The resulting well-depth $D_{xc} = E(R_\mathrm{e}) - E(R_{xc}) = 0.281$ eV relative to the lowest crossing with the threshold curve (here,

$R_{xc} = R_x(1^4\Sigma_u^+, 1^3\Sigma_u^+))$ approximately equals the electron affinity of $1^4\Sigma_u^+$. Its shallow well ($\omega_e = 166$ cm^{-1}) causes a relatively large spread between R_e and $R_0 = \langle \chi_{v=0}, R\,\chi_{v=0}\rangle = 6.64a_0$. Around the equilibrium, $1^4\Sigma_u^+$ is almost exclusively governed by the configuration that arises from the ground state by the excitation $2\sigma_g \rightarrow 3\sigma_g$. The adiabatic and the vertical electron affinities for $1^4\Sigma_u^+$, both taken relative to the "parent" state $1^3\Sigma_u^+$, are not much different, *viz.* $\text{EA}_a(1^4\Sigma_u^+) = 0.246$ eV (CINO) or 0.257 eV (CINOQ) and $\text{EA}_v(1^4\Sigma_u^+) = 0.274$ eV (CINO) or 0.281 eV (CINOQ). These values are slightly larger than the electron affinity $\text{EA}_a(1^4\Pi_g) = 0.233$ eV of the lowest metastable quartet state $1^4\Pi_g$ of He_2^-, also taken relative to $1^3\Sigma_u^+$ of He_2 [36].

At its equilibrium, the state $1^4\Sigma_u^+$ is located 8906 cm^{-1} or 1.10 eV above the corresponding bottom of the doublet continuum (determined by the $\text{X}^1\Sigma_g^+$ PEC at $R_e(1^4\Sigma_u^+)$). For increasing R this vertical energy difference decreases (see Fig. 2) until just before the $1^4\Sigma_u^+$ state is absorbed into the quartet continuum the $1^4\Sigma_u^+$ PEC hits and tracks the $\text{X}^1\Sigma_g^+$ curve within ≈ 100 cm^{-1} (*i.e.*, within the absolute errors of the calculations). If only limited by electronic decay *via* the quartet continuum, the $1^4\Sigma_u^+$ PEC could support about 17 vibrational levels for $^7\text{Li}_2^-$ and rotational quantum number $J = 0$. However, rather than by the electronic continuum, the vibrational motion is affected more strongly by the crossing between the $1^4\Sigma_u^+$ and $1^4\Pi_g$ PECs at $R_x(1^4\Sigma_u^+, 1^4\Pi_g) = 5.43a_0$ such that for smaller R the latter PEC becomes the lower one. As a consequence, vibrational $1^4\Sigma_u^+$ levels with $v \geq 5$ are destabilized by electronic dipole transitions to $1^4\Pi_g$.

Compared with the $1^4\Sigma_u^+$ PEC, the well and the discrete part of the $1^4\Pi_g$ PEC is shifted toward shorter internuclear separations. In particular, the minimum of the $1^4\Pi_g$ PEC is attained for a bond length $R_e = 5.90a_0$ that is about $0.6a_0$ shorter than for $1^4\Sigma_u^+$, and the $1^4\Pi_g$ state is absorbed into the quartet continuum at a distinctly smaller distance $R_x(1^4\Pi_g, 1^3\Sigma_u^+) = 8.20a_0$. This is obviously related to the replacement of the $3\sigma_g$-orbital for $1^4\Sigma_u^+$ by a stronger binding $1\pi_u$-orbital in the configuration governing $1^4\Pi_g$. According to the standard prescription of populating molecular orbitals, for systems up to and including N_2 the $1\pi_u$-orbital would yield a lower energy than the $3\sigma_g$-orbital. For Li_2^- these energy levels are inverted, similar to the situation of He_2^- in its lowest quartet state $1^4\Pi_g$. For Li_2^-, the electron affinity of $1^4\Pi_g$ (again relative to the parent state $1^3\Sigma_u^+$) $\text{EA}_a(1^4\Pi_g) = 0.163$ eV is somewhat smaller than that for $1^4\Sigma_u^+$, and the $1^4\Pi_g$ PEC can support only 8 vibrational levels below the quartet continuum. Nevertheless, since the crossing with the $1^4\Sigma_u^+$ PEC already occurs at an energy $T_x \approx 113$ cm^{-1} above the $1^4\Pi_g$ minimum, only the vibrational ground state of $1^4\Pi_g$ escapes strong perturbations by that crossing. At the corresponding $R_0 = 5.93a_0$, our computations predict a relatively long lifetime $\approx 2\times10^{-2}$ s of $1^4\Pi_g$ against radiative transitions to $1^4\Sigma_u^+$. The vibrational wave functions of excited states $v > 0$ extend beyond the crossing point $R_x(1^4\Sigma_u^+, 1^4\Pi_g)$ into the region where $1^4\Pi_g$ is stable, thus causing a delay of the vibronic transitions to $1^4\Sigma_u^+$. As already mentioned, also the excited $1^4\Sigma_u^+$ vibrational motion is perturbed by that crossing; in additional to the usual decay *via* vibrational cascading, for $R < R_x(1^4\Sigma_u^+, 1^4\Pi_g)$ the nonvanishing dipole transition probability with lifetimes from 10^{-2} to 10^{-4} s for $1^4\Sigma_u^+$ also renders de-excitation *via* (repeated) vibronic transitions $(1^4\Sigma_u^+, v'') \leftrightarrow (1^4\Pi_g, v')$ possible. The ordering $1^4\Sigma_u^+ < 1^4\Pi_g < 1^4\Pi_u$ with respect to increasing relative stability was proposed by Meng *et al.* [35] for the low-lying Be_2^+ quartet states, where on the domain of principal interest (R from 3 to $8a_0$) the $1^4\Pi_u$ PEC lies distinctly (≥ 0.5 eV) above the $1^4\Pi_g$ PEC. Hence, it should come as no surprise that – as a result of our computations – for Li_2^- this state does not exist as a discrete state below the quartet continuum. A similar conclusion holds for the purely repulsive $1^4\Sigma_g^+$ PEC.

Finally, for separations R less than $R_x(1^4\Pi_g, 1^4\Sigma_g^-) = 3.57a_0$, the other state displayed in Figure 3, namely $1^4\Sigma_g^-$, supplants $1^4\Pi_g$ as the energetically lowest quartet state for Li_2^-. For the cation, $1^4\Sigma_g^-$ was classified as a doubly excited state with strongest relative binding reported so far for Be_2^+ [35]. In the case of Li_2^-, the $1^4\Sigma_g^-$ PEC emerges from the quartet continuum at a point in the immediate vicinity of the crossing $R_x(1^3\Sigma_u^+, 1^3\Pi_u) = 4.82a_0$ between the triplet PECs $1^3\Sigma_u^+$ and $1^3\Pi_u$ of Li_2 (*cf.* Fig. 3). Whereas the shape of the $1^4\Sigma_g^-$ PEC indicates that its minimum should not be far from the absorption point, the part where $1^4\Sigma_g^-$ exists as a discrete state below the quartet continuum is purely repulsive. The radiative decay of $1^4\Sigma_g^-$ into $1^4\Sigma_u^+$ or $1^4\Pi_g$ is dipole forbidden; nonetheless, the interactions with the threshold states of the quartet continuum can be expected to prevent metastability of $1^4\Sigma_g^-$. For sufficiently short internuclear separations, the $1^4\Sigma_g^-$ PEC represents the lowest Li_2^- energies, converging to the atomic ground state $^4\text{S}^o$ in the UAL.

From the low-lying quartet states of He_2^-, the states $1^4\Phi_g$ and 1^4I_g were predicted to be (meta)stable; both states were characterized by configurations with two electrons in orbitals of similar level of diffuseness attached to a He_2^+ ground state core. Also the Li_2^- quartet states considered here can be expressed in an analogous way as a Li_2^+ ground state core $1\sigma_g^2 1\sigma_u^2 2\sigma_g$ plus two valence electrons. An alternative interpretation starts from the Li_2 triplet core; then the states $1^4\Sigma_u^+$ and $1^4\Pi_g$ result from addition of the bonding orbitals $3\sigma_g$ and $1\pi_u$, respectively, leading to positive electron affinities, whereas the state $1^4\Sigma_g^+$ arises from addition of the antibonding $3\sigma_u$-orbital.

6 Conclusions

The prediction of possibly metastable quartet states $1^4\Sigma_u^+$ and $1^4\Pi_g$ for Li_2^- is the main result of our computations; in particular, $1^4\Sigma_u^+$ is a candidate for a long-lived state that could be observable by mass spectroscopic methods. The PECs for both quartet states have their respective minimum below the quartet continuum, but are absorbed into that continuum for small or large internuclear separations. Furthermore, since they are embedded into the doublet continuum, spin-orbit, spin-spin, or similar small interactions not included in our calculations, prevent absolute stability of these quartet states. Such interactions, however, are usually rather small for anions and light nuclei. In addition, many intercombination transitions with $\varDelta S = \pm 1$ are also forbidden by other, approximate or rigorous, selection rules; for instance, the rigorous rule $u \not\leftrightarrow u$ does not allow electronic dipole transitions between $1^4\varSigma_u^+$ and $X^2\varSigma_u^+$. The most important decay channel for $1^4\varSigma_u^+$ will be pre-ionisation by interaction with continuum doublet states of Li_2^-. In particular, the leading order contribution should be the direct relativistic term [37] of the Breit-Pauli matrix element between $1^4\varSigma_u^+$ and $X^2\varSigma_u^+$ (interactions with $1^2\varPi_u$ are not very favourable because the real part of the PEC intersects the $1^4\varSigma_u^+$ PEC at $R_x(1^4\varSigma_u^+, 1^2\varPi_u) \approx 7.42a_0$ with small Frank-Condon factors). Whereas this suggests lifetimes of order milli- or microseconds as a crude estimate for the metastability of the state $1^4\varSigma_u^+$, a precise quantitative treatment will be an interesting task for future investigations.

Our theoretical predictions are based on the non-relativistic Schrödinger equation, but the relativistic corrections for the calculated spectroscopic quantities should be distinctly smaller than the errors caused by incomplete basis set, basis superposition error, size-inconsistency and deviations in the extrapolation procedure of the employed computational method. The discussion in Section 3 motivates the following error bars for Li_2: $\pm 0.01a_0$ for R_e (± 0.2 in the exceptional case of $1^3\varSigma_u^+$), ± 0.02 eV for D_e, ± 250 cm^{-1} for T_e, or ± 4 cm^{-1} for ω_e (± 6 cm^{-1} in the case of $1^3\varSigma_u^+$). Although in case of Li_2^- the accuracy is reduced, we do not expect error bars more than twice as large as those for Li_2. On the other hand, an improvement of our results by independent calculations with enhanced accuracy and employing computing sources beyond those available for this study might be desirable. Also an investigation of higher spin states in Li_2^- should be of interest.

The critical reading of the manuscript by S. Farley is gratefully acknowledged. A substantial part of this work was done while enjoying the kind hospitality at the CPT, Marseille, and useful technical assistance for the computations was provided by the Rechenzentrum der Universität Hildesheim.

References

1. P.H. Blustin, J.W. Linnett, J. Chem. Soc. Faraday Trans. **70**, 826 (1974).
2. H.W. Sarkas, S.T. Arnold, J.H. Hendricks, V.L. Slager, K.H. Bowen, Z. Phys. D **29**, 209 (1994).
3. E. Anderson, J. Simons, J. Chem. Phys. **64**, 4548 (1976).
4. D.A. Dixon, J.L. Gole, K.O. Jordan, J. Chem. Phys. **66**, 567 (1977).
5. R. Shepard, K.D. Jordan, J. Simons, J. Chem. Phys. **69**, 1788 (1978).
6. H. Partridge, C.W. Bauschlicher, P.E.M. Siebahn, Chem. Phys. Lett. **97**, 198 (1983).
7. D.D. Konowalow, J.L. Fish, Chem. Phys. Lett. **104**, 210 (1984).
8. K.K. Sunil, K.D. Jordan, Chem. Phys. Lett. **104**, 343 (1984).
9. H.H. Michels, R.H. Hobbs, L.A. Wright, Chem. Phys. Lett. **118**, 67 (1985).
10. M. Gutowski, J. Simons, J. Chem. Phys. **101**, 4867 (1994).
11. R. Poteau, F. Spiegelmann, J. Mol. Spectrosc. **171**, 299 (1995).
12. H. Hogreve, J. Phys. B **31**, L439 (1998).
13. C. Blondel, Phys. Scripta T **58**, 31 (1995).
14. M.W. McGeoch, R.E. Schlier, Phys. Rev. A **23**, 1708 (1986).
15. T. Sommerfeld, L.S. Cederbaum, Phys. Rev. Lett. **80**, 3723 (1998).
16. G. Das, A.C. Wahl, J. Chem. Phys. **44**, 87 (1966); G. Das, J. Chem. Phys. **46**, 1568 (1967).
17. M.L. Olson, D.D. Konowalow, Chem. Phys. **21**, 393 (1977).
18. M.L. Olson, D.D. Konowalow, Chem. Phys. **22**, 29 (1977).
19. M.M. Hessel, C.R. Vidal, J. Chem. Phys. **70**, 449 (1979).
20. D.D. Konowalow, M.L. Olson, J. Chem. Phys. **71**, 450 (1980).
21. B. Jonsson, B.O. Roos, P.R. Taylor, P.E.M. Siegbahn, J. Chem. Phys. **74**, 4566 (1981).
22. D.D. Konowalow, J.L. Fish, Chem. Phys. **84**, 463 (1984).
23. I. Schmidt-Mink, W. Müller, W. Meyer, Chem. Phys. **92**, 263 (1985).
24. U. Kaldor, Chem. Phys. **140**, 1 (1990).
25. S. Evangelisti, G.L. Bendazzoli, L. Gagliardi, Int. J. Quant. Chem. **55**, 277 (1995).
26. R. Poirier, R. Kari, I.G. Csizmadis, *Handbook of Gaussian Basis Sets* (Elsevier, Amsterdam, 1985).
27. I. Fischer, V.E. Bondybey, P. Rosmus, H.J. Werner, Chem. Phys. **151**, 295 (1991).
28. R.J. Buenker, in *Proceedings of the Workshop om Quantum Chemistryand Molecular Physics*, Wollong, Australia, 1982; in *Studies in Physical and Theoretical Chemistry*, **21** Current Aspects of Quantum Chemistry, edited by R. Carbo (Elsevier, New York, 1982).
29. S.R. Langhoff, E.R. Davidson, Int. J. Quant. Chem. **7**, 999 (1973).
30. M.M. Hessel, C.R. Vidal, J. Chem. Phys. **70**, 4439 (1979).
31. J. Vergés, R. Bacis, B. Barakat, P. Carrot, S. Churassy, P. Crozet, Chem. Phys. Lett. **98**, 203 (1983).
32. F. Engelke, H. Hage, Chem. Phys. Lett. **103**, 203 (1983).
33. R.A. Bernheim, L.P. Gold, P.B. Kelly, T. Tipton, D.K. Veirs, J. Chem. Phys. **76**, 57 (1982).
34. H. Hogreve, Chem. Phys. Lett. **187**, 479 (1992).
35. B. Meng, P.J. Bruna, J.S. Wright, Molec. Phys. **79**, 1305 (1993).
36. H.H. Michels, Phys. Rev. Lett. **52**, 1413 (1984).
37. G. Miecznik, T. Brage, C. Froese Fischer, Phys. Rev. A **47**, 3718 (1993).